

Non-linear transport and heat dissipation in metallic carbon nanotubes

Marcelo A. Kuroda¹ and Jean-Pierre Leburton²

¹*Beckman Institute and Department of Physics, University of Illinois at Urbana-Champaign, Illinois 61801*

²*Beckman Institute and Department of Electrical and Computer Engineering,
University of Illinois at Urbana-Champaign, Illinois 61801*

(Dated: July 19, 2018)

We show that the local temperature dependence of thermalized electron and phonon populations along metallic carbon nanotubes is the main reason behind this non-linear transport characteristics in the high bias regime. Our model that considers optical and zone boundary phonon emission as well as absorption by charge carriers is based on the solution of the Boltzmann transport equation that assumes a local temperature along the nanotube, determined self-consistently with the heat transport equation. By using realistic transport parameters, our results not only reproduce experimental data for electronic transport, but also provide a coherent interpretation of thermal breakdown under electric stress. In particular, electron and phonon thermalization prohibits ballistic transport in short nanotubes.

PACS numbers: 73.63.Fg, 73.23.-b, 65.80.+n

Carbon nanotubes (CN) are one-dimensional (1D) nanostructures that have stimulated broad research interest because of their unique electrical versatility into semiconductors and metals, depending of their chirality [1]. From a technological viewpoint, their remarkable electrical and mechanical properties make them promising materials for applications in high performance nanoscale electronic and mechanical devices [2, 3]. Among these properties, the interrelation between electronic and thermal transport in these quasi 1D structures is particularly interesting. Early experiments on non-linear transport in metallic single walled nanotubes (m-SWNTs) using low resistance contacts revealed current saturation at the $25\mu\text{A}$ level, which was attributed to the onset of electron backscattering by high energy optical (OP) and zone boundary (ZB) phonons in the high bias regime [4]. More recently, series of independent high-field transport measurements on various length m-SWNTs demonstrated the absence of current saturation with current levels over $60\mu\text{A}$ in short samples ($\lesssim 55\text{nm}$), which was interpreted as ballistic transport along the CN [5, 6]. Among the findings was also the observation of thermal breakdown and burning under high electric stress. In the mean time, the electrical conductance of multi-walled nanotubes (MWNTs) under high bias has shown step-like decrease caused by the successive burning of the CN outer shells [7, 8]. In these experiments CNs burn unexpectedly at mid-length under stress even on a substrate and on the presence of a back gate in a field effect device geometry [9]. Despite various attempts to model these systems [4, 5, 6], up to now no coherent interpretation has emerged that reconciliates heat dissipation with electronic transport and describes thermal effects in m-CN under electric stress.

In this letter, we show that the non-linear characteristics of metallic CNs find their origin in the non-homogeneous Joule heating along the nanotube, which is

caused by the thermalized distribution of electrons scattered by high energy phonons, even in short m-SWNT. We specifically show that Joule heating is maximum at CN mid-length and, owing to the 1D nature of the structure, increases drastically with the CN length, resulting in thermal breakdown at lower bias than in shorter CNs. Our model is based on the Boltzmann transport equation with OP and ZB phonon scattering and solved self-consistently with the heat transfer equation, providing a coherent interpretation of electric and thermal transport in m-SWNTs in agreement with experimental data [5, 6]. In particular we show that the high current level in short CNs is not due to ballistic transport but to reduced Joule heating.

We use the linear dispersion relation of electronic states around the Fermi level ($\epsilon(k) = \pm \hbar v_F k$) [10], being v_F the Fermi velocity. Thus, the Boltzmann equation reads:

$$v_F \partial_x f^\alpha(\epsilon) + \frac{eF}{\hbar} \partial_k f^\alpha(\epsilon) = C_{ph}^\alpha(I, T) \quad (1)$$

Here $f^\alpha(\epsilon)$, F , e and C_{ph} are the distribution function for the α energy branch, the electric field, the electron charge and the electron-phonon collision integral, respectively. The index α denotes the energy branches with positive (+) and negative (-) Fermi velocity in the first (1) and second valleys (2) of the m-CN. In metallic systems high electron density and strong inter-carrier scattering thermalizes the electron distribution. We therefore assume that the electron distribution function $f^\alpha(\epsilon)$ obeys Fermi-Dirac statistics with a local electronic temperature $T_{el}(x)$:

$$f^\alpha(\epsilon) = 1/(1 + \exp((\epsilon - \epsilon_F^\alpha)/k_B T_{el}(x))) \quad (2)$$

where ϵ_F^α is the quasi Fermi level of branch α . As a result, the collision integral C_{ph}^α also depends on the position. We neglect acoustic phonons that are only relevant in the low bias regime, and consider the contribution of high

density OP and ZB phonons [11, 12] that play a central role in energy dissipation in the high bias regime. As illustrated in Fig. 1(a), the different processes (inter- and intra-branch) considered in C_{ph} include both the emission and absorption of these phonons with energy ($\hbar\omega_{op} \approx 0.2\text{eV}$) much larger than thermal fluctuations at room temperature. Each of these phonons contributes to the collision integral as follow:

$$C_{ph}^\alpha(I, T(x)) = \sum_{i, \beta} \left\{ \frac{R_e^i}{\pi} [f^\beta(k)(1-f^\alpha(k-q)) - f^\alpha(k)(1-f^\beta(k-q))] + \frac{R_a^i}{\pi} [f^\beta(k)(1-f^\alpha(k+q)) - f^\alpha(k)(1-f^\beta(k+q))] \right\} \quad (3)$$

where the Greek letter index β runs over the two branches and two valleys, i stands for OP and ZB phonons and R_e^i (R_a^i) is the phonon emission (absorption) rate. Hence the first (second) two terms in Eq. 3 corresponds to processes involving the emission (absorption) of a phonon limited by Pauli exclusion principle. For instance, the first term describes a process in which an electron scatters from a state in branch β with momentum k to a state in branch α with momentum $k-q$ by emitting a phonon. In all these processes, both total energy and momentum are conserved. The emission and absorption rate coefficients are given by:

$$R_a^i(T_L) = \frac{N_q}{\tau_i} = \frac{1}{\tau_i} \frac{1}{\exp(\hbar\omega/k_B T_L) - 1} \quad (4)$$

$$R_e^i(T_L) = \frac{N_q + 1}{\tau_i} = R_a \exp(\hbar\omega/k_B T_L) \quad (5)$$

where T_L is the lattice temperature and $1/\tau_i$ stands for the bare scattering rate for OP and ZB phonons that we assume to be independent of carrier energy in a first approximation. In computing the collision integral, we make the key ‘‘ansatz’’ that electrons and lattice are in local thermal equilibrium (i.e. $T_L = T_L(x) = T_{el}(x)$). We define the electron density as:

$$n_\alpha = \frac{1}{\pi} \int_{-k(E_c)}^{+\infty} f^\alpha(k) dk \quad (6)$$

where E_c is the bottom of the conduction band, and the current to be:

$$I = e(n_+ - n_-)v_F \quad (7)$$

where the $+$ ($-$) index corresponds to the branches with positive (negative) Fermi velocity. Then integrating Eq. 1 over the momentum for each branch, and properly accounting for different branches, we obtain:

$$v_F \partial_x (n^+ - n^-) = 0 \quad (8)$$

$$v_F \partial_x (n^+ + n^-) - \frac{2eF}{\pi\hbar} = 2 \int dk C_{ph}(I, T(x)) = 2\tilde{C}_{ph}(I, T(x)) \quad (9)$$

Eq. 8 is the expression of the current conservation in the system which by symmetry $\epsilon_{F1}^\pm = \epsilon_{F2}^\pm$ and with charge neutrality in the CN yields $\epsilon_{F(1,2)}^+ = -\epsilon_{F(1,2)}^-$. Integrating Eq. 9 over the length of the nanotube L , and assuming equal electron densities at the contacts, we find the voltage drop V_{DS} along the nanotube given by:

$$V_{DS} = -\frac{\pi\hbar}{e} \int_{-L/2}^{L/2} dx \tilde{C}_{ph}(I, T(x)) \quad (10)$$

This equation implicitly depends on the current and the temperature profile along the nanotube, and must be solved self-consistently with the heat transport equation to obtain both current and temperature profile.

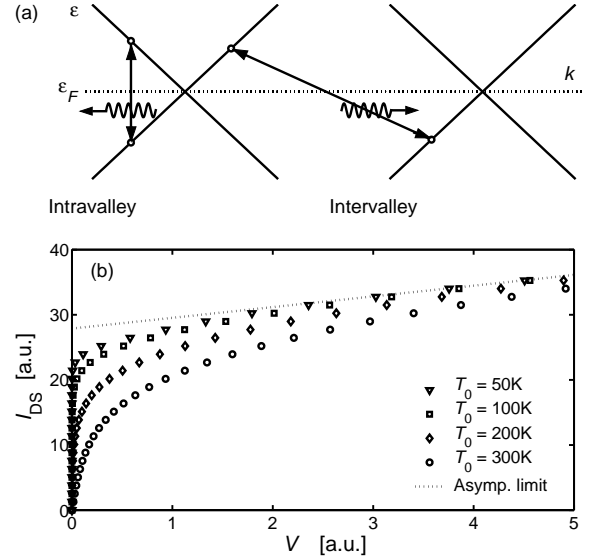


FIG. 1: (a) Scattering processes considered in the calculations. The intravalley (left) and intervalley (right) transitions with emission and absorption of optical phonons are included. (b) IV characteristics for different constant temperatures along the tube. Dashed line: asymptotic behavior for all temperatures in the high bias regime.

As a particular case, it is interesting to compute the IV relation from Eq. 10 by assuming only OP phonon scattering at constant temperature (i.e. $T(x) = T_0$) in the CN. The results are plotted in Fig. 1(b) where the high bias regime exhibits an asymptotic behavior independent of temperature which is given by:

$$V_{DS}(I) = \frac{1}{G_0} \frac{L}{v_F \tau_{op}} (I - I_{\omega_{op}}) \quad (11)$$

where $I_{\omega_{op}} = e\omega_{op}/\pi$ is the threshold current, corresponding to the onset of electron backscattering by OP phonons [4] and $G_0 = 2e^2/h$ is the quantum conductance. We point out that Eq. 11 is not consistent with the current interpretation of electrons accelerated ballistically in the electric field until acquiring enough energy to emit a phonon, but rather results from the imbalance between the population of the energy branches with positive and

negative Fermi velocities. By considering ZB phonons, the voltage drop in the m-SWNT is a linear combination of expressions similar to Eq. 11, which would still result in a threshold current, but with a more complicated expression.

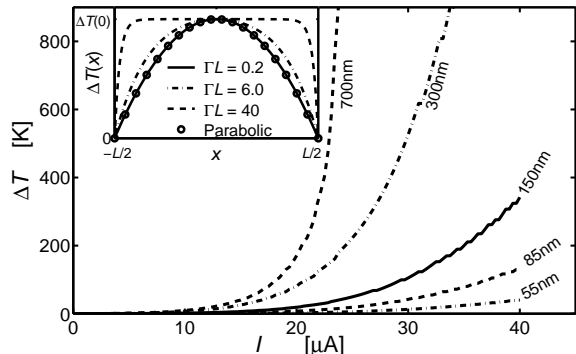


FIG. 2: Temperature difference between the middle of the tube and the leads as a function of the current for different CN lengths [5]. Inset: Temperature profile along the NT for different values of ΓL .

When heating effects become relevant, thermal dissipation is taken into account self-consistently with Eq. 10. We consider that two mechanisms for the heat dissipation: i) diffusion through the supporting substrate (if the CN stands on one), and ii) flow through the contacts. Hence, defining $\Delta T = T(x) - T_0$ (where T_0 is the temperature of the substrate and leads), the heat equation becomes [13]:

$$-\kappa \frac{d^2 \Delta T}{dx^2} + \gamma \Delta T = q^* \quad (12)$$

where κ is the thermal conductivity, γ is the coupling coefficient with the substrate and q^* is the power dissipated per unit volume. Here we make the usual approximation that process (i) is proportional to the local temperature difference between CN and substrate. In our calculations both the thermal conductivity and the coupling coefficient are assumed to remain constant along the tube. The coefficient γ is given [13] by:

$$\gamma = \frac{\kappa_{sub}}{td} \quad (13)$$

where κ_{sub} , t and d are the thermal conductivity of the substrate, the diameter of the nanotube and the thickness of substrate, respectively. We also assume that the power is homogeneously generated along the CN and given by Joule's law:

$$q^* = jF \quad (14)$$

where $j = I/A$ is current density through the effective cross section A and the electric field F is given by $F = |V_{DS}/L|$. Then the solution for temperature profile is given by:

$$\Delta T(x) = \frac{q^*}{\gamma LS} \left[1 - \frac{\cosh(\Gamma x)}{\cosh(\Gamma L/2)} \right] \quad (15)$$

where $\Gamma = \sqrt{\gamma/\kappa}$.

Different scenarios can take place depending on the value ΓL (see the inset of Fig. 2). On the one hand, for $\Gamma L \ll 1$ diffusion through the substrate is negligible and the temperature profile exhibits a parabolic shape. On the other hand, for $\Gamma L \gg 1$, heat basically dissipates through the substrate and the temperature is almost constant along the CN. This latter situation occurs in long tubes strongly coupled to the substrate. In any case, the highest temperature point is at the middle of the tube.

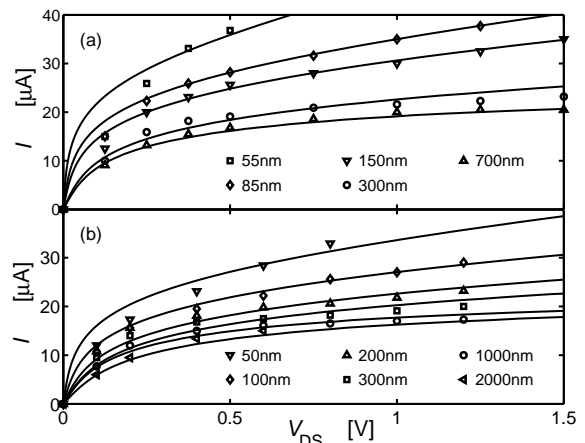


FIG. 3: Comparison between theoretical and experimental IV characteristics for different CN lengths: (a) Ref. [5] (b) Ref. [6].

In our calculations we use $T_0 = 300\text{K}$. The energies of OP and ZB phonons are $\hbar\omega_{op} = 0.20\text{eV}$ and $\hbar\omega_{zb} = 0.16\text{eV}$, respectively. We use the standard accepted value for the thermal conductivity κ (30W/cmK) [14] and $\Gamma = 10^{11}\text{W cm}^{-3}\text{K}^{-1}$. Fig. 2 shows the temperature difference in the middle of the tube ($\Delta T(0)$) as a function of I for different CN length, corresponding to the data of Ref. [5]. The longer the nanotube, the faster the rise in temperature as the threshold current is overcome. This is due to the fact that dissipation occurs over a longer distance while heat removal mainly takes place at the contacts in 1D structures. Estimates for the breakdown temperature correspond to 800°C [15]. Therefore, short tubes are expected to carry larger currents before thermal breakdown. As shown in Fig. 3, the results for the IV characteristics are in good agreement with the experimental data [5, 6]. Deviations in the low bias regime are mainly due to the absence of acoustic phonons scattering in our model. For the sake of simplicity, we assume relaxation times for OP and ZB phonons with equal values, which are $\tau = (13 \pm 2)\text{fs}$ for the first [5] and $\tau = (6.9 \pm 1.5)\text{fs}$ for the second [6] sets of experimental data. The difference between the two values could be due to the fact that CNs may have different diameters with different phonons spectra (breathing modes) [16] in each case, and contact quality. Nevertheless, the obtained mean free paths (between 6nm and 10nm) are consistent with experimental

previous estimates [5, 6]. For long tubes (i.e. $L=700\text{nm}$ in the first case [5] and for $L \geq 1000\text{nm}$ in the second case [6]), we need to increase in both cases the relaxation times to $(27 \pm 3)\text{fs}$ to fit the experimental data. Since dissipation is considerably stronger in long CNs, these longer times may be associated to the emergence of non-linear thermal effects in m-SWNT thermal conductivity not taken into account in Eq. 12, and for which the temperature and geometry dependence at room temperature or higher remains an open issue [17, 18].

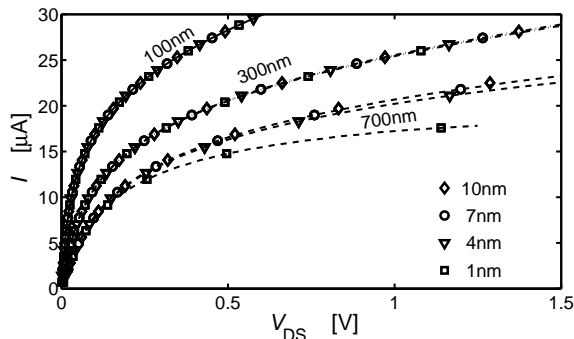


FIG. 4: IV characteristics for different tube lengths and diameters. Short tubes (100nm and 300nm) are practically independent of the diameter, while in the long tube (700nm), deviations appear for the small diameter (1nm).

Finally, Fig. 4 shows the IV -characteristics obtained for CNs of different diameters and lengths, assuming that both the thermal conductivity and the relaxation time are equal among tubes. Despite this strong assumption, the relevant issue to emphasize here is the weak dependence of the IV characteristics on the size of the CN. Appreciable deviations can be observed only in 700nm tube (dashed line) for small diameters ($\sim 1\text{nm}$). This weak relation is consistent with the interpretation of Collins et al. [7, 8] for the electrical breakdown under electrical stress observed in MWNTs, where different layers in a MWNT (separated by about 0.4nm) carry similar currents in the high bias regime. The breakdown of successive carbon layers produces approximately constant diminutions of the current in the high bias regime because IV characteristics are geometry independent. Moreover, the highest temperature arises at the CN mid-length (inset of Fig. 2) and therefore, electrical breakdown is, as experimentally observed, expected to take place there too.

In conclusions, we have shown that the consideration of a thermalized electron distribution in local equilibrium with a non-homogenously heated lattice through OP and ZB scattering determined self-consistently by the current level account for the non-linear IV characteristics

of the m-SWNTs in the high bias regime. The magnitude of the temperature variation as a function of the CN lengths is consistent with the occurrence of thermal breakdown at mid-length for long CN under electrical stress. While the dependence of thermal conductivity on temperature still remains under investigation, our self-consistent model provides a coherent picture of the onset of thermal effects with electronic transport in m-SWNT.

The authors are indebted to A. Cangelaris for fruitful discussion. This work was supported by the Beckman Institute for Advance Science and Technology and NSF - Network of Computational Nanotechnology.

-
- [1] R. Saito, G. Dresselhaus, and M. Dresselhaus, “*Physical Properties of Carbon Nanotubes*,” Imperial College Press (1998).
 - [2] P.L. McEuen, M.S. Fuhrer, Hongkun Park, IEEE Transactions on Nanotechnology, **1**, 78 (2002).
 - [3] Ph. Avouris, J. Appenzeller, R. Martel, S. Wind, Proceedings of the IEEE, **91**, (1772) 2003.
 - [4] Z. Yao, C. L. Kane, and C. Dekker, Phys. Rev. Lett. **84**, 2941 (2000).
 - [5] A. Javey, J. Guo, M. Paulsson, Q. Wang, D. Mann, M. Lundstrom, and H. Dai, Phys. Rev. Lett. **92**, 106804 (2004).
 - [6] J.Y. Park, S. Rosenblatt, Y. Yaish, V. Sazonova, H. Üstünel, S. Braig, T.A. Arias, P.W. Brouwer, P.L. McEuen, Nano Lett. **4**, 517 (2004).
 - [7] P.G. Collins, M. Hersam, M. Arnold, R. Martel, and Ph. Avouris, Phys. Rev. Lett. **86**, 3128 (2001).
 - [8] P.G. Collins, M.S. Arnold, P. Avouris, Science **292**, 706 (2001).
 - [9] R.S. Muller, T.I. Kamins, “*Device Electronics for Integrated Circuits*”, 3rd. Edition, John Wiley & Sons (2002).
 - [10] R.A. Jishi, D. Inomata, K. Nakao, M.S. Dresselhaus, G. Dresselhaus, J. Phys. Soc. Japan, **63**, 2252 (1994).
 - [11] R. Saito, T. Takeya, T. Kimura, G. Dresselhaus and M.S. Dresselhaus, Phys. Rev. B **57**, 4145 (1998).
 - [12] V. Perebeinos, J. Tersoff, and Ph. Avouris, Phys. Rev. Lett. **94**, 027402 (2005).
 - [13] C. Durkan, M.A. Schneider, and M.E. Welland, J. Appl. Phys. **86**, 1280 (1999).
 - [14] J. Che, T. Cagin, and W.A. Goddard III, Nanotechnology, **11**, 65 (2000).
 - [15] M. Radosavljevic, J. Lefebvre, and A. T. Johnson, Phys. Rev. B **64**, 241307(R) (2001).
 - [16] B.J. LeRoy, S.G. Lemay, J. Kong and C. Dekker, Nature **432**, 371 (2004).
 - [17] T. Yamamoto, S. Watanabe, and K. Watanabe, Phys. Rev. Lett. **92**, 075502 (2004).
 - [18] J.X. Cao, X.H. Yan, Y. Xiao, and J.W. Ding, Phys. Rev. B **69**, 073407 (2004).